

Nanoscale imaging with an integrated system combining stimulated emission depletion microscope and atomic force microscope

YU JianQiang, YUAN JingHe, ZHANG XueJie, LIU JianLi & FANG XiaoHong*

Beijing National Laboratory for Molecular Sciences, Key Laboratory of Molecular Nanostructure and Nanotechnology, Institute of Chemistry, Chinese Academy of Sciences, Beijing 100190, China

Received March 27, 2013; accepted May 27, 2013; published online August 13, 2013

We have built an integrated imaging system by combining stimulated emission depletion (STED) microscope and atomic force microscope (AFM). The STED microscope was constructed based on the supercontinuum fiber laser and a super lateral resolution of 42 nm was achieved. With this integrated imaging system, morphological features, mechanical parameters and fluorescence super resolution imaging were obtained simultaneously for both nanobeads and fixed cell samples. This new integrated imaging system is expected to obtain comprehensive information at the nanoscale for studies in nanobiology and nanomedicine.

stimulated emission depletion (STED) microscope, atomic force microscope (AFM), confocal microscope, integrated imaging, super-resolution imaging

Citation: Yu J Q, Yuan J H, Zhang X J, et al. Nanoscale imaging with an integrated system combining stimulated emission depletion microscope and atomic force microscope. *Chin Sci Bull*, 2013, 58: 4045–4050, doi: 10.1007/s11434-013-6011-z

For centuries, optical techniques have been playing an important role in life sciences, and about 80% of all microscopy investigations are carried out with optical microscopes [1]. Taking advantage of the optical transparency of cells, optical microscopy provides noninvasive imaging of the interior of cells in three dimensions. Moreover, it allows the detection of specific cellular constituents, such as proteins, through fluorescence tagging, and the monitoring of their dynamic changes. Recent years have seen increasing efforts in the integration of optical microscopy with other advanced microscopic techniques, such as atomic force microscopy (AFM), to obtain comprehensive information for the characterization of biological samples [2,3]. With its capability of working in solution, AFM has been widely used as a multifunctional molecular tool in biological studies. AFM can not only provide high resolution morphological imaging at the nanometer scale in biologically relevant aqueous environments, but also measure mechanical properties of protein and strength of biomolecular bonds. Furthermore, using

the AFM tip as a manipulation tool allows the precise and controllable modification of biological systems from the level of cells down to individual molecules [4,5]. Combining optical microscope, especially fluorescence microscope, with AFM technique is becoming an important tool in the study of morphological and mechanical changes of the specifically labeled molecules or cellular components for a better understanding of biological process.

Several examples of integrating fluorescence microscope and AFM have been reported over the last few years, such as, the integration of total internal reflection fluorescence microscope (TIRFM) with AFM [6], and confocal optical microscope with AFM [7,8]. However, due to the barrier of diffraction limit for all lens-based optical microscopes [9], the incompatible imaging resolution of fluorescence microscopy (sub micrometer) and AFM (sub nanometer) hindered their wider applications.

In recent years, several strategies have been developed to overcome the diffraction barrier and preserve the advantages of far-field fluorescence microscopy [10–13]. Among them, stimulated emission depletion (STED) microscopy [10,14–17]

*Corresponding author (email: xfang@iccas.ac.cn)

stands out by its ability to instantly provide signal from selected nanosized regions, which makes it particularly suitable for fast imaging. In STED microscope, a laser beam (STED beam) is required to overlay a regular excitation beam (Exc beam) to de-excite fluorophores by stimulated emission. The STED beam produces a doughnut-shaped focal pattern, featuring a “zero”-intensity point in its center, thus it inhibits fluorescence emission everywhere except at the center of the focus. Therefore, the effective fluorescence volume was confined to subdiffraction size. Scanning the co-aligned STED beam and Exc beam through the sample, or vice versa, yields super-resolution images.

Integration of the newly developed STED microscope with AFM will lead to a promising nanoscope for nanobiology and nanomedicine. Harke et al. [18] recently reported such an integrated system based on two pulse lasers for excitation and depletion. In this work, we presented a flexible integration system by combining STED microscope and AFM with a simpler technique for wavelength selecting and timing measurement. In the system, a supercontinuum laser source was used to provide both Exc and STED beams, so the temporal synchronization is automatically achieved. Another advantage of using supercontinuum laser is that it can generate low average power due to the low pulse repetition frequency, which could protect the fragile biological specimens from being photodamaged. Moreover, as the optical image and AFM image were obtained separately in the previous reported STED/AFM system [18], we have achieved, for the first time, that the optical signal and force signal are acquired simultaneously at each pixel during the sample scanning in our integrated STED/AFM. Super-resolution

STED imaging and simultaneous AFM imaging of nano-beads as well as biological samples have been demonstrated.

1 Materials and methods

1.1 Setup of the integrated system

As shown in Figure 1, the integrated system was based on combining a commercial AFM instrument (BioScope Catalyst, Bruker, USA) with a home-built STED microscope that was constructed following the basic design in the previous report [14]. The STED microscope was equipped with a supercontinuum laser (Fianium, Southampton, UK), which covers the spectrum region from 500 to 1750 nm, and provides both excitation and the STED pulses. The fundamental pulse width of the laser is about 350 ps, and the optical power at the back aperture of the objective lens can reach 30 μ W for the Exc beam and 1.2 mW for the STED beam at a repetition rate of 1 MHz.

To realize the STED imaging, firstly the infrared region ($\lambda > 842$ nm) of the super continuum spectrum was stripped from the whole spectrum with a short pass filter (Semrock, New York, USA). Then the two orthogonally polarized beams were established using a broadband polarizing beam splitter cube (CVI, Albuquerque, USA). The s-polarized beam was used for excitation whereas the p-polarized beam for STED.

According to the absorption and emission spectrum of the fluorescent dye ATTO565 (Sigma-Aldrich, Shanghai, China) used in our experiments, the wavelength of the excitation and STED were determined at 532 and 650 nm

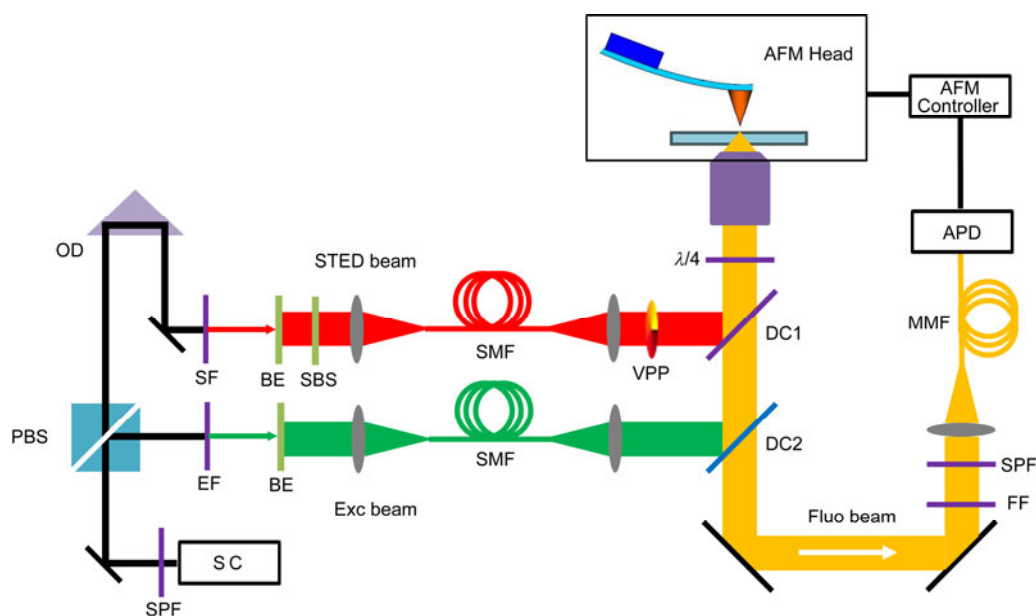


Figure 1 Schematic diagram of the integrated imaging system. SC, supercontinuum laser; SPF, short pass filter; OD, optical delay; PBS, polarizing beam splitter; EF, excitation filter; SF, STED filter; BE, beam expander; SBS, STED beam shutter; SMF, single mode fibers; VPP, vortex phase plate; DC, dichroic mirrors; FF, fluorescence filter; MMF, multimode fiber; APD, avalanche photodiode detector.

respectively. Hereby, we used band pass filters to extract both the Exc beam and the STED beam by use of excitation filter (FF01-530, Semrock, New York, USA) and STED filter (FF01-650, Semrock, New York, USA). The pulse duration of the excitation and STED was measured to be 351 ± 60 ps and 312 ± 28 ps respectively, as determined by a high-speed photoreceiver (New Focus, CA, USA) that was connected to a digital phosphor oscilloscope (Tektronix, Beaverton, USA). The optical delay line was used to adjust the interval between the excitation pulse and the STED pulse. Based on our calculation [19], the appropriate interval between the excitation pulse and the STED pulse should be about 100 ps.

To create a focal doughnut, the STED beam passed through a vortex phase plate (RPC Photonics, Rochester, NY, USA) with a helical phase ramp of 2π to modulate the wavefront. Then both the Exc and STED beams passed through an achromatic quarter wave plate (THORLABS, New Jersey, USA) to make them polarizing circularly.

Both Exc and STED beams were separately coupled into polarization-maintaining single mode optical fibers (THORLABS, New Jersey, USA) after they were expanded by the two beam expanders. The fiber outputs were collimated and collinearly coupled into an oil immersion objective lens (UPlanSApo, 100X, Olympus, Japan) using two dichroic mirrors (Chroma, Vermont, USA), the fluorescence signal was collected by the same objective lens and separated from the excitation and STED beams by these two dichroic mirrors and an additional fluorescence band pass filter (FF01-582, Semrock, New York, USA). A short pass filter (FF01-680, Semrock, New York, USA) was used to prevent the AFM work laser line (850 nm) from interfering the optical channel.

The collected fluorescence was focused into a multimode optical fiber (50 μm , THORLABS, New Jersey, USA) which acted as a confocal pinhole of 1.22 times the size of an Airy disk. The fluorescence photons were registered with an avalanche photodiode module (Perkin Elmer, Vaudreuil, Quebec, Canada) which was connected to the Digital I/O port of the AFM controller (NanoScope V, Bruker, USA). The image acquisition was performed by scanning the sample with a commercial AFM head (BioScope Catalyst, Bruker, USA) mounted on a commercial microscopic stand (IX71, Olympus, Japan). The STED and confocal images were obtained by opening and closing the STED beam shutter. Typically, images of $10 \mu\text{m} \times 10 \mu\text{m}$ were acquired with 10 nm pixel size and 1–2 ms dwell times on each pixel. The STED and confocal images were displayed and analyzed by using the counting channel of the Nanoscope software (NanoScope 8.10, Bruker, USA), the restored STED images with blind deconvolution algorithm were obtained using a self-compiling MATLAB program.

1.2 Nanobead immobilization

To prepare the nanobead sample for the integrated STED/

AFM imaging, the microscope cover slips were firstly cleaned by sonication in detergent, acetone, and 1 mol/L KOH for 30 min respectively, rinsed with mini-Q water three times after each step, and then dried by nitrogen. The diluted (10^{-5} fold dilution) fluorescent polystyrene nanobeads ($\Phi 40$ nm FluoSpheres orange, Invitrogen, Paisley, UK) were dropped onto the cleaned cover slip, and then dried by nitrogen.

1.3 Cell culture and staining

Human embryonic kidney HEK 293 cells (HEK 293 cells) and Human cervical carcinoma cells (CaSki cells) were used in this study. The cells were cultured with Dulbecco's modified Eagle's medium (DMEM, Gibco, Grand Island, New York, USA) supplemented with 10% fetal bovine serum (Hyclone, Omaha, Nebraska, USA) at 37°C in a 5% CO_2 incubator. The cells were plated in 30-mm confocal-specific culture dishes (Corning, Steuben County, New York, USA) which were previously coated by sterilized 0.1 mg/ml poly-D-lysine solution (Sigma-Aldrich). When the cells grew to 70%–80% confluence, they were fixed and stained for actin filament. For actin filament staining, cells were washed with PBS, permeabilized in PBS containing 0.5% Triton X-100 for 10 min, fixed with 4% formaldehyde in PBS for 20 min, and then treated with phalloidin-ATTO565 (Sigma-Aldrich, Shanghai, China) for 15 min.

2 Results and discussions

2.1 Super-resolution imaging with STED

A home-built STED microscope was used for the integrated STED/AFM system. Different from the reported STED/AFM integrated system, several updating techniques were applied to make the STED microscope easier to implement and more stable. The supercontinuum fiber laser was used as it can supply almost all of wavelengths for the fluorescence excitation and STED. The energy of the laser is larger than 1 nJ/nm, satisfying the power request for STED microscope. Moreover, the excitation and STED pulses are inherently synchronous, and thus the timing shift between the excitation and STED pulse is avoided. To check the interval between the excitation pulse and STED pulse, a super-speed digital oscillograph was used, which simplifies the procedure of timing adjustment.

To validate the super-resolution imaging capability of our STED microscope, we imaged the samples of 40 nm fluorescent nanobeads, Figure 2 shows the comparison between the confocal image and STED image at the same sample region. The closely spaced nanobeads which are not resolved in the confocal image (Figure 2(a), insert) are clearly discernible in the STED image (Figure 2(b), insert)

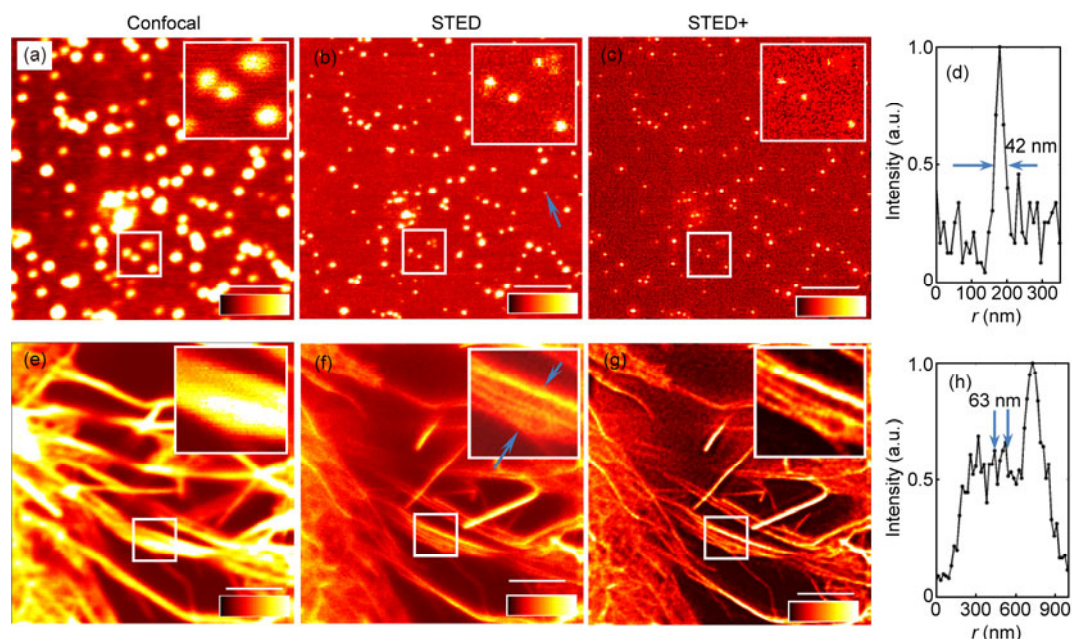


Figure 2 Super-resolution imaging of the nanobeads with the STED microscope. The confocal image (a), STED image (b) and deconvolution of the STED image (c) of nanobeads. (d) Line profiles of the beads (pointed by blue arrowhead in (b)). The confocal image (e), STED image (f) and deconvolution of the STED image (g) of the actin filaments. (h) Line profiles of the actin filaments (between blue arrowheads in (f)). The insets in (a), (b) and (c) correspond to the white rectangle regions respectively. Bar, 2 μm .

and the STED image restored with blind deconvolution algorithm (Figure 2(c), insert). The intensity profile of the nanobeads shows a 42 nm in full width at half maximum (FWHM). This resolution is even higher than that in the previously reported STED imaging of the same sample (50–60 nm) [14].

We further imaged the actin filaments in the filopodium of the HEK 293 cells (Figure 2(e)–(g)). The five distinct actin filaments (in the white rectangle regions) are clearly shown in the STED image (Figure 2(f), insert) and the restored STED image with blind deconvolution algorithm (Figure 2(g), insert), but they cannot be resolved in the confocal counterpart (Figure 2(e), insert). Profiles of these actin filaments (Figure 2(h), insert) indicate that 63 nm spacing (the narrowest spacing in Figure 2(h)) between the filaments can be well resolved. Therefore, super-resolution imaging of the biological sample is also realized in our STED microscope.

The results demonstrate that a high-quality STED microscope based on a supercontinuum laser system has been successfully built, with an all-optical lateral resolution of better than 40 nm considering the broadening effect by the bead diameter. Different from confocal fluorescence microscopy, STED microscopy has a more compatible resolution with the resolution of AFM for cells, thus is more suitable for the integrated imaging by optical microscope and AFM. Taking the advantage of emitting a whole spectrum of visible light from the supercontinuum laser source, this STED microscope can easily be applied to different fluorescent tagged examples by just selecting appropriate dichroic

mirrors and fluorescence filters.

2.2 Imaging of nanobeads with the integrated system

With the home-built STED microscope, we then integrated it with the commercial AFM to have the fluorescence signal collection and sample scanning all controlled by the AFM controller. Two modes of STED/AFM imaging can be mainly used in our integrated system. In the first mode, so called simultaneous imaging model, optical signal and force signal are obtained at each pixel during the sample scanning, thus the same area of the sample can be imaged by STED microscope and AFM simultaneously. In the second mode, which is called targeting imaging mode, a large area of the sample can be firstly imaged by STED microscope to find a small region of interest, then the morphological features of the region of interest is obtained by AFM. As we known, it is difficult for AFM to get very fine features in a large area, especially for fluctuant surfaces such as cells, whereas the STED imaging is advantageous. The targeting mode makes use of the advantages of both STED microscope and AFM, and will be a powerful tool in biological studies.

The performance of our integrated STED/AFM system was checked by imaging the fluorescent nanobeads using the above-mentioned two modes. As shown in Figure 3, we firstly scanned a larger area (20 $\mu\text{m} \times 20 \mu\text{m}$) with the STED microscope to find a region of interest (the white rectangle, Figure 3(a)). Then, the height (Figure 3(e)) and force volume (Figure 3(f)) of the region was measured with the AFM. The STED image (Figure 3(b)) and the confocal image

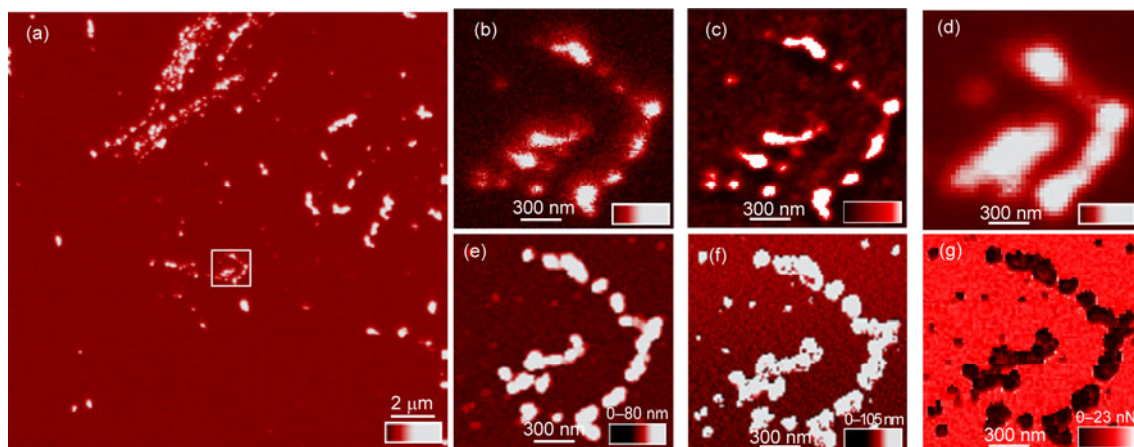


Figure 3 Integrated STED/AFM imaging of nanobeads. (a) STED super-resolution imaging in a large area. (b) STED image of the region in the white rectangle in (a). (c) Deconvolution of the STED image. (d) Confocal image. (e) AFM morphological image. (f) AFM force volume imaging. (g) AFM force adhesion mapping.

(Figure 3(d)) were simultaneously acquired too. The force adhesion (Figure 3(g)) of the same region was obtained by processing the force volume data at the same time.

Both STED image and its restored image with blind deconvolution (Figure 3(c)) show fine details of the separated nanobeads, demonstrating a higher resolution than the confocal image where only the rough profile of the area is displayed. The AFM images (Figure 3(e)–(g)) show the morphological features which is in agreement with the STED image. Individual and clustered fluorescent beads can be identified in the STED and AFM images but not in the confocal microscope. More particles could be found in the AFM images as some non-fluorescent particles in the AFM image, cannot be discerned in the STED image. The results demonstrated that simultaneous imaging mode and targeting imaging mode were both realized. Fluorescence imaging, morphological features and mechanical parameter of the fluorescent polystyrene nanobeads can be obtained simultaneously. Super-resolution fluorescence imaging can also guide the AFM tip more precisely to the target parts of the sample.

2.3 Imaging of the actin filament with the integrated system

We further applied our integrated system to the imaging of the actin filaments in the filopodium of CaSki cells. Comparing to the confocal image of the actin filaments (Figure 4(a)), the STED image (Figure 4(c)) and its deconvolution image (Figure 4(d)) show the finer features of the actin filaments in the same area. The morphological image of the filopodium was obtained by AFM (Figure 4(b)). Some intertwined structures can be resolved more clearly in STED images and the AFM image, but cannot be discerned in the confocal image.

Therefore, the cellular actin filament is imaged with the integrated STED/AFM system, for the first time, to obtain

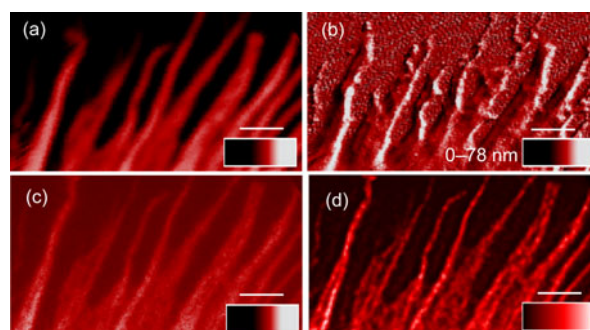


Figure 4 Integrated STED/AFM imaging of the filopodium. (a) Confocal image. (b) AFM morphological image. (c) STED image. (d) The deconvolution of the STED image. Bar, 1 μm .

super resolution fluorescence image and morphological features simultaneously at the nanoscale. The results demonstrate that the integrated imaging can be realized for cell study.

In summary, an integrated imaging system combining STED microscope and AFM has been built. The STED microscope has shown a high lateral resolution which is compatible to that of AFM. With the integrated system, super resolution fluorescence imaging, morphological features and mechanical parameter of the fluorescently stained samples can be obtained simultaneously. The integrated STED/AFM system is expected to offer a new tool in nanobiology and nanomedicine for the characterization of biological samples at the nanoscale.

This work was supported by the National Basic Research Program of China (2013CB933701), the National Natural Science Foundation of China (91213305, 21127901, 21121063), and Chinese Academy of Sciences.

- Hell S W. Far-field optical nanoscopy. *Science*, 2007, 316: 1153–1158
- Binnig G, Quate C F, Gerber C. Atomic force microscope. *Phys Rev Lett*, 1986, 56: 930–933

- 3 Siebena C, Kappel C, Zhu R, et al. Influenza virus binds its host cell using multiple dynamic interactions. *Proc Natl Acad Sci USA*, 2012, 109: 13626–13631
- 4 Shi X, Zhang X, Xia T, et al. Living cell study at the single-molecule and single-cell levels by atomic force microscopy. *Nanomedicine*, 2012, 7: 1625–1637
- 5 Yuan S, Dong Z L, Miao L, et al. Research on the reconstruction of fast and accurate AFM probe model. *Chin Sci Bull*, 2010, 55: 2750–2754
- 6 Nishida S, Funabashi Y, Ikai A. Combination of AFM with an objective-type total internal reflection fluorescence microscope (TIRFM) for nanomanipulation of single cells. *Ultramicroscopy*, 2002, 91: 269–274
- 7 Kassies R, Van Der Werf K O, Lenferink A, et al. Combined AFM and confocal fluorescence microscope for applications in bio-nanotechnology. *J Microsc-Oxford*, 2005, 217: 109–116
- 8 Kondra S, Laishram J, Ban J, et al. Integration of confocal and atomic force microscopy images. *J Neurosci Meth*, 2009, 177: 94–107
- 9 Abbe E. Beitrage zur Theorie des Mikroskops und der mikroskopischen Wahrnehmung. *Archive f Mikroskop Anat*, 1873, 9: 413–468
- 10 Hell S W, Wichmann J. Breaking the diffraction resolution limit by stimulated emission: Stimulated-emission-depletion fluorescence microscopy. *Opt Lett*, 1994, 19: 780–782
- 11 Rust M J, Bates M, Zhuang X W. Sub-diffraction-limit imaging by stochastic optical reconstruction microscopy (STORM). *Nat Method*, 2006, 3: 793–795
- 12 Pohl D W, Denk W, Lanz M. Optical stethoscopy-image recording with resolution $\lambda/20$. *Appl Phys Lett*, 1984, 44: 651–653
- 13 Hell S W, Kroug M. Ground-state-depletion fluorescence microscopy: A concept for breaking the diffraction resolution limit. *Appl Phys B*, 1995, 60: 495–497
- 14 Wildanger D, Rittweger E, Kastrop L, et al. STED microscopy with a supercontinuum laser source. *Opt Express*, 2008, 16: 9614–9621
- 15 Liu Y J, Ding Y C, Alonas E, et al. Achieving $\lambda/10$ resolution CW STED nanoscopy with a Ti: Sapphire oscillator. *PLoS One*, 2012, 7: 1–9
- 16 Kuang C F, Zhao W, Wang G R. Far-field optical nanoscopy based on continuous wave laser stimulated emission depletion. *Rev Sci Instrum*, 2010, 81: 053709
- 17 Deng S H, Liu L, Cheng Y, et al. Effects of primary aberrations on the fluorescence depletion patterns of STED microscopy. *Opt Express*, 2010, 18: 1657–1666
- 18 Harke B, Chacko J, Haschke H, et al. A novel nanoscopic tool by combining AFM with STED microscopy. *Opt Nanoscopy*, 2012, 1: 1–6
- 19 Yu J, Yuan J, Fang X, et al. Effects of excitation and depletion process on resolution of stimulated emission depletion microscope (in Chinese). *Acta Optica Sinica*, 2010, 30: S100405

Open Access This article is distributed under the terms of the Creative Commons Attribution License which permits any use, distribution, and reproduction in any medium, provided the original author(s) and source are credited.